Impact of Viscous Dissipation on MHD Darcy-Forchheimer Nanoliquid Flow Comprising Gyrotactic Microorganisms past a Nonlinear Extending Surface

Maria Batool[1*], Shaheen Akhter[2], Sohail Ahmad[3], Kashif Ali[4] and Muhammad Ashraf[5]

[1, 2, 3, 5] *Center for Advanced Studies in Pure and Applied Mathematics (CASPAM), Bahauddin Zakariya University, Multan 60800, Pakistan*

[2] *Department of Mathematics, COMSATS University (Islamabad), Sahiwal, Pakistan*

[3, 4] *Department of Basic Sciences and Humanities, Muhammad Nawaz Sharif University of Engineering and Technology, Multan 60000, Pakistan;*

Corresponding author email: *maria.batool34@yahoo.com*

Cell No: *+923336001058*

Abstract

In the current article, MHD flow problem of Darcy-Forchheimer nanoliquid comprising motile microorganisms with viscous dissipation impact past a nonlinear elongated sheet is addressed. The inclusion of gyrotactic microorganisms in nanoliquid assists to boost up the thermal efficiency in numerous micro-biological systems. Iterative solution of the single-phase flow problem is attained by utilizing the procedure of SOR (Successive over Relaxation). The influences of leading parameters on flow velocity, temperature, density and concentration of motile microbes are considered and depicted through tables and graphs by employing software of MATLAB. Furthermore, comparison table is developed to check the accuracy of numerical results of the flow problem under consideration. An increment in the Forchheimer parameter causes reduction in the velocity distribution. It is portrayed that the Lewis number and Brownian motion parameter tend to enhance the rate of mass transport.

Keywords: Darcy-Forchheimer; Bioconvection; Viscous Dissipation; Nonlinear Stretching Sheet; Gyrotactic Microorganisms.

2010 Mathematics Subject Classification: 76A05; 76M20, 35Q35, 76D05, 80A20

Abbreviations:

u	$x-$Component of velocity
v	$y-$Component of velocity
μ	Dynamic viscosity
υ	Kinematic viscosity
ρ_{Fl}	Fluid's density
ρ_{Np}	Nanoparticles' density
T	Temperature
c_p	Specific heat
b_o	Positive constant
K_*	Permeability of medium
c_B	Drag force coefficient
D_{Tp}	Thermophoresis diffusion coefficient
D_{Bm}	Brownian coefficient
D_{Gm}	Microorganism diffusion coefficient
σ_{Ec}	Electric conductivity
T_{Inf}	Ambient temperature
W_{cs}	Maximum swimming speed of cell
T_{bn}	Temperature at surface of sheet
b_{ch}	Chemotaxis constant
α	Thermal diffusivity
Ec	Eckert number
B_0	Strength of magnetic field
n	Microorganisms' concentration
C	Volume fraction of nanoparticles
Me	Magnetic parameter
$\Pr$	Prandtl number
Le	Lewis number
Sc	Schmidt number
Nb	Parameter of Brownian motion
Nt	Parameter of thermophoresis
Pe	Peclet number
λ	Porosity parameter
η	Dimensionless variable
Fr	Forchheimer parameter

1. Introduction

The nanoliquid has well known contributions in the fields of medicine, chemical processes, devices of heat transfer, chillers, cooling systems and industry etc. Initially, Choi [1] introduced that combined mixture of micro metallic particles and conventional base fluids form a new kind of liquid, known as nanoliquid. This new type of engineering liquid has more capacity of heat transfer as compared to conventional base fluids. When Reynolds number is greater than 1 then the flow is nonlinear. In such circumstances, it becomes impossible to ignore impacts of inertia. The non-Darcian model of permeable media is obtained from classical Darcian model that includes inertial drag, vorticity diffusion impacts, inertial drag and their combination as well. In order to demonstrate the impressions of boundary as well as inertia, Forchheimer [2] developed a square velocity term which is added in expression of velocity. Muskat [3] called this term as "Forchheimer term" which is valid for high Reynolds number. Darcy-Forchheimer theory was utilized by Seddeek [4] to investigate mixed convection Darcy-Forchheimer flow with thermophoresis and viscous dissipation impact through porous media. The solution of problem involving flow of Darcy-Forchheimer Maxwell nanoliquid was revealed by Sajid et al. [5] on a stretching linear shallow with support of shooting technique. Sheikholeslami et al. [6-8] numerically interpreted the nanofluid performance in a solar LFR system, heat storage with honeycomb configuration utilizing nanoparticles and solar system equipped with innovative hybrid nanofluid.

Darcy- Forchheimer viscous nanofluid flow past an elongating curved surface was analyzed by Saif et al. [9] through a penetrable region. Nasir et al. [10] investigated flow problem of thin film 2D Darcy-Forchheimer nanofluid past a flat unsteady stretchable surface in a porous media. Problem of micropolar 3D MHD (magnetohydrodynamics) Darcy-Forchheimer nanoliquid CNTs flowing among horizontal & parallel plates was inspected in a porous region by Khan et al. [11]. Ganesh et al. [12] scrutinized MHD Darcy-Forchheimer flow of nanofluid past a sheet in thermally stratified porous medium. They solved the flow problem by employing Runge-Kutta method of order four with shooting technique. Nanoliquid flow with thermophoresis impact and Brownian motion is numerically examined by Hayat et al. [13] under Darcy-Forchheimer relationship. Sadiq and Hayat [14] addressed the problem of MHD Darcy-Forchheimer two-dimensional flow due to a stretched surface.

The boundary-layer MHD flow of Maxwell nanoliquid generated by a stretching surface was investigated by Muhammad et al. [15] in a porous medium under influence of uniform magnetic field. Hayat et al. [16] scrutinized the boundary layer flow problem of Darcy-Forchheimer Williamson nanomaterial on a bidirectional nonlinearly stretching surface in a porous region. They adopted the Homotopy Analysis Method (HAM) to generate the numerical solution for governing nonlinear system of flow problem. Zakaullah et al. [17] computed the numerical solution of Darcy-Forchheimer nanofluid flow problem with partial slip impacts with assistance of shooting methodology. Moreover, they explored that temperature and concentration of nanoparticles have expanding behaviors for larger values of Forchheimer parameter. Turk and Tezer-Sezgin [18] addressed the flow problem of micropolar nanoliquid inside a square under impact of magnetic field and computed its numerical solution by employing Finite Element Method (FEM). Shafiq et al. [19] inspected special impacts of thermal slip and Arrhenius activation energy in flow of Darcy-Forchheimer nanoliquid due to a stretching surface. Some of the investigations involving Darcy-Forchheimer flow have been published [20-22].

The swimming of gyrotactic microorganisms generates the phenomena of bioconvection. The spectacle of bioconvection boosts up microscale mixing and stability of nanoparticles. Effective distribution of heat is due to stabilized nanoparticles. Shahid et al. [23] numerically inspected the flow of blood comprising motile microbes passing through a stretching and penetrable region. They computed the numerical solution ofblood flow problem by employing methodology of Successive Taylor Series Linearization (STSLM). Waqas et al. [24] envisaged Buongiorno's model to investigate flow characteristics of MHD Williamson nanoliquid due to a porous wedge containing gyrotactic microorganisms. The numerical solution of this time-dependent flow problem was achieved by shooting method. In the presence of motile microorganisms, the numerical solution of flow problem involving Maxwell nanofluid with thermal radiation impact was obtained by Sohail and Naz [25] with the assistance of HAM. Some recent relevant studies can be referred to the refs. [26-29].

The present study of Darcy-Forchheimer nanofluid flow has different valuable applications in biomedical sciences and biotechnology. According to our knowledge, no work on the numerical investigation of viscous dissipation in Darcy-Forchheimer nanofluid flow comprising gyrotactic microbes employing SOR (Successive over Relaxation) technique has been done yet. This fact encouraged us to conduct the current study. This paper is concerned with behavior of numerous parameters on the MHD flow of Darcy-Forchheimer nanoliquid containing gyrotactic microorganisms under influence of viscous dissipation. The numerical solutions are clarified with the help of figures and tables of various pertinent parameters involved in the concerned problem through MATLAB.

2. Mathematical Formulation

Let us assume steady viscous 2D incompressible Darcy-Forchheimer flow of MHD nanofluid due to a stretching sheet which behaves nonlinearly. The sheet has motion along $x-axis$ with stretching velocity of form $U_{bn} = b_o x^m$, where m and $b_o > 0$ are constant terms.

The geometry of the modeled flow problem is given below in Fig. 1:

The system of differential equations representing the current flow problem has form:

$$\frac{\partial u}{\partial x}+\frac{\partial v}{\partial y}=0 \tag{1}$$

$$u\frac{\partial u}{\partial x}+v\frac{\partial u}{\partial y}=\nu\left(\frac{\partial^2 u}{\partial y^2}\right)-\left(\frac{\sigma_{Ec}B_o^2x^{m-1}}{\rho_{Fl}}+\frac{\nu}{K_*}\right)u-\frac{c_B}{\sqrt{K_*}}u^2 \tag{2}$$

$$u\frac{\partial T}{\partial x}+v\frac{\partial T}{\partial y}=\alpha\frac{\partial^2 T}{\partial y^2}+\frac{(\rho c)_{Np}}{(\rho c)_{Fl}}\times\left\{D_{Bm}\left(\frac{\partial C}{\partial y}\frac{\partial T}{\partial y}\right)+\frac{D_{Tp}}{T_{Inf}}\left(\frac{\partial T}{\partial y}\right)^2\right\}+\frac{\nu}{c_p}\left(\frac{\partial u}{\partial y}\right)^2 \tag{3}$$

$$u\frac{\partial C}{\partial x}+v\frac{\partial C}{\partial y}=D_{Bm}\frac{\partial^2 C}{\partial y^2}+\frac{D^{Tp}}{T_{Inf}}\frac{\partial^2 T}{\partial y^2} \tag{4}$$

$$u\frac{\partial n}{\partial x}+v\frac{\partial n}{\partial y}+\frac{b_{ch}W_{cs}}{(C_{bn}-C_{Inf})}\left\{\frac{\partial}{\partial y}\left(n\frac{\partial C}{\partial y}\right)\right\}=D_{Gm}\frac{\partial^2 n}{\partial y^2} \tag{5}$$

The boundary conditions (BCs) related to above equations are:

$$u=U_{bn}=b_ox^m,\quad v=0,\quad T=T_{bn},\quad C=C_{bn},\quad n=n_{bn}\quad \text{at } y=0 \tag{6}$$

$$u\to 0,\quad T\to T_{Inf},\quad C\to C_{Inf},\quad n\to n_{Inf}\quad \text{as}\quad y\to\infty \tag{7}$$

Let’s define dimensionless quantities

$$\eta=\frac{1}{2}\sqrt{\frac{2b_o(m+1)\rho_{Fl}}{\mu}}x^{\frac{m-1}{2}}y,\quad \theta(\eta)=\frac{T-T_{Inf}}{T_{bn}-T_{Inf}},\quad \chi(\eta)=\frac{n-n_{Inf}}{n_{bn}-n_{Inf}},$$
$$\phi(\eta)=\frac{C-C_{Inf}}{C_{bn}-C_{Inf}},\quad u=b_ox^mf'(\eta),\quad v=-\frac{1}{2}\sqrt{2b_o(m+1)\nu}x^{\frac{m-1}{2}}. \tag{8}$$

The velocity components $u=\frac{\partial\psi}{\partial y}$ & $v=-\frac{\partial\psi}{\partial x}$ provide assistance to develop stream function ψ and η denotes the dimensionless similarity variable. The components u and v help to satisfy Eq. (1) in form of ψ. The transformation specified in (8) can be exploited to convert Eqs. (2) – (5) into ODEs given below:

$$f''' + ff'' - \left[\frac{2m}{m+1}\right] f'^2 - Me^2 f' - \lambda f' - Fr(f')^2 = 0, \tag{9}$$

$$\theta'' + \Pr\left[Nb\theta'\phi' + Nt\theta'^2 + \theta' f \right] + \Pr Ecf''^2 = 0, \tag{10}$$

$$\phi'' + \frac{Nt}{Nb}\theta'' + Le\Pr(f'\phi') = 0, \tag{11}$$

$$\chi'' + Sc(f\chi') - Pe\left[\chi'\phi' + \phi''(\chi + \sigma)\right] = 0, \tag{12}$$

Also, BCs written in (6) as well as (7) have dimensionless form:

$$f(0) = 0, \quad f'(0) = 1, \quad \theta(0) = 1, \quad \phi(0) = 1, \quad \chi(0) = 1, \text{ at } \eta = 0, \tag{13}$$

$$f' = 0, \quad \theta = 0, \quad \phi = 0, \quad \chi = 0, \text{ as } \eta \to \infty \tag{14}$$

Where primes symbolize derivative w.r.t η. Further, Me is magnetic parameter, Le is Lewis number, Nt is thermophoresis parameter, λ is porosity parameter, Ec shows Eckert number, $\Pr$ is Prandtl number, Sc is Schmidt number, Nb is parameter of Brownian motion, Pe signifies Peclet number, σ_{Ec} is a constant term, Fr is the Forchheimer parameter, which have mathematical forms as:

$$Nt = \frac{(\rho c)_{Np} D_{Th}(T_{bn} - T_{Inf})}{(\rho c)_{Fl}\, \upsilon T_{Inf}}, \qquad Nb = \frac{(\rho c)_{Np} D_{Bm}(C_{bn} - C_{Inf})}{(\rho c)_{Fl}\, \upsilon}, \qquad \Pr = \frac{\upsilon}{\alpha},$$
$$Ec = \frac{(u_{bn})^2}{c_p(T_{bn} - T_{Inf})}, \qquad Sc = \frac{\upsilon}{D_{Gm}}, \qquad Le = \frac{\upsilon}{D_{Bm}}, \qquad Me = \sqrt{\frac{2\sigma_{Ec} B_o^2}{b_o \rho_{Fl}(m+1)}}, \tag{15}$$
$$Pe = \frac{b_{ch} W_{cs}}{D_{Gm}}, \qquad \sigma_{Ec} = \frac{n_{Inf}}{(n_{bn} - n_{Inf})}, \qquad \lambda = \frac{2\upsilon}{K_* b_o (m+1) x^{m-1}}, \qquad Fr = \frac{2c_B x}{K_*^{\frac{1}{2}}(m+1)}.$$

3. Numerical Computation

Many researchers are contributing in various fields to find numerical solutions of nonlinear modeled problems. In our problem, the numerical elucidation of resulted nonlinear ODEs (9)-(12) involving BCs described in (13)-(14) is accomplished with the assistance of a methodology based on SOR. We have adopted this procedure because it provides the facility of fast convergence. Since, it is complicated to compute analytical solution of nonlinear differential equations of higher order. A detail discussion on our numerical technique can be seen in our prior papers [30-35].

To find numerical solution of coupled system of nonlinear ODEs, we applied Finite Difference Method. As the ODE given in (9) is of order 3, its order is reduced by putting $f' = r$. Finally, the resultant system of equations with their boundary conditions has form:

$$r'' + fr' - \left[\frac{2m}{m+1}\right] r^2 - Me^2 r - \lambda r - Fr(r)^2 = 0, \tag{16}$$

$$\theta'' + \Pr\left[Nb\theta'\phi' + Nt\theta'^2 + \theta' f\right] + \Pr Ecr'^2 = 0, \tag{17}$$

$$\phi'' + \frac{Nt}{Nb}\theta'' + Le\Pr(f\phi') = 0, \tag{18}$$

$$\chi'' + Sc(f\chi') - Pe\left[\chi'\phi' + \phi''(\chi + \sigma_{Ec})\right] = 0, \tag{19}$$

The boundary conditions get the form:

$$\begin{aligned} &f(0) = 0, \quad r(0) = 1, \quad \theta(0) = 1, \quad \phi(0) = 1, \quad \chi(0) = 1, \quad at \quad \eta = 0, \\ &r = 0, \qquad \theta = 0, \qquad \phi = 0, \qquad \chi = 0, \qquad as \qquad \eta \to \infty \end{aligned} \tag{20}$$

Firstly, the domain $[0, \infty)$ of flow problem under observation is discretized for the numerical manipulation of above-mentioned system of equations. In order to integrate the equation $f' = r$, Simpson's numerical iterative process is employed. Additionally, well-known central difference approximation is employed to discretize the involved derivatives in (16)-(20) as well as an iterative solution is found by applying the methodology of SOR. This iterative scheme is terminated when

$$\max\left(\left\|r_{j+1} - r_j\right\|_2, \left\|f_{j+1} - f_j\right\|_{2,} \left\|\theta_{j+1} - \theta_j\right\|_{2,} \left\|\phi_{j+1} - \phi_j\right\|_{2,} \left\|\chi_{j+1} - \chi_j\right\|_2\right) < Tol_{itr}$$

is satisfied up to four consecutive iterations.

4. Results and Discussion

In this section, we are committed to present our outcomes through physical elucidations. The relevant flow model dimensionless equations (9)-(12) are numerically treated with the help of SOR method. The velocity $f'(\eta)$, motile microorganisms (microbes) density distribution $\chi(\eta)$, concentration $\phi(\eta)$ and temperature $\theta(\eta)$ display asymptotic appearance against the well-adjusted step size η. The movements of microorganisms and nanoparticles are independent of each other. The motion of nanoparticles is because of the Brownian and thermophoresis effects while bioconvection phenomenon within the flow causes the motion of the mobile microorganisms. The microorganisms own self-propelled movement unlike the nanoparticles. The impact of the physical parameters on the shear stress, mass transport rate, motile microbes' density number and heat transport rate are also examined and tabularized.

The motile microbes' density, velocity, concentration and temperature profiles are drawn in Figs. 2-5 respectively for multiple values of magnetic field parameter Me. It can be evidently seen from these figures that the effect of magnetic parameter enhances microorganisms' density, temperature and concentration while its effect on velocity shows a decreasing trend. A retarding force is induced in the direction of motion because of the applied magnetic field. This force strictly opposes the motion which causes a reduction in the velocity of fluid. The same profiles are examined for porosity parameter, as appeared in Figs. 6-9. It is obvious from the analysis of these figures that the porosity and magnetic parameters insert the same effects on the aforementioned profiles.

The impacts of local inertia or Forchheimer parameter on the profiles such as $f'(\eta)$, $\chi(\eta)$, $\theta(\eta)$ and $\phi(\eta)$ are portrayed in Figs. 10-13. The velocity profile gets decrease with the influence of Forchheimer parameter while the remaining profiles (microbes' density, concentration and temperature) are increased with an increment in this parameter. Both parameters (porosity and Forchheimer) act parallel to each other in terms of their effects on the dimensionless profiles. The porosity of the medium and the surface drag are proportional to the Forchheimer parameter or inertial coefficient. Due to this reason the resistive force increases which causes an enhancement in surface friction. Consequently, the raising values of Fr cause a decrement in the velocity and increment in the motile microbe's density.

A numerical data comparison, to validate our code, is presented in Table 1. The outcomes are correlated with those presented by Rasool et al. [36]. The results are matched in limiting cases for distinct values of Forchheimer parameter. A better correlation of the results in Table 1 assures the accuracy of our numerical solutions.

Tables 2-5 are provided to check out the impacts of the preeminent parameters on local motile density number $\chi'(0)$, local Sherwood number $\phi'(0)$, skin friction coefficient $f''(0)$ and local Nusselt number $\theta'(0)$. The variation of skin friction for several parameters is depicted in Table 2. It is noticed here that various values of porosity, magnetic and Forchheimer parameters cause an enhancement in the skin friction. The impacts of parameters like Nt, Nb, λ, Fr, Ec and Me on the Nusselt number can be examined in Table 3. The values of $\theta'(0)$ are diminishing with the influence of these parameters. The magnetic, porosity and thermophoresis parameters tend to devaluate the mass transport rate on the sheet surface, on the other hand; the Lewis number, Brownian motion parameter and the Forchheimer parameter cause a substantial increase in the Sherwood number (mass transfer rate) as portrayed in Table 4.

The desired consequences can be attained by providing the suitable values to the preeminent parameters. The pores sizes can affect the local density number of microorganisms. If the sizes of pores are so small such that the tiny organisms do not cross them easily then the bioconvection may not occur. In order to avoid this situation, it will be better to take medium having high porosity or much smaller permeability. Table 5 reveals the influences of Me, λ, Pe, Sc and Fr over the motile microorganisms density number $\chi'(0)$. The density of microbes is enhanced with the escalating values of Pe, Sc and Fr. Contrarily, the magnetic and the porosity parameter tend to decline the density of the microbes. In the tabular analysis, it is worth mentioning that the surface drags as well as $\chi'(0)$ is increased on the surface of sheet with the influence of the Forchheimer parameter.

Conclusions:

We have numerically investigated the MHD Darcy-Forchheimer nanofluid flow due to nonlinear elongating sheet in a porous medium. Magnetic effects not only maintain the temperature but also regulate flow. The numerical outcomes are attained via the Successive over Relaxation method. Major findings are specified below:

- It has been elucidated that the magnetic parameter tends to enhance microorganisms' density, temperature and concentration while its impact on flow velocity demonstrates a declining trend.
- An increase in Forchheimer parameter causes a decrement in the velocity and increment in the motile microbe's density.
- It is portrayed that the porosity and thermophoresis parameters tend to devaluate the mass transport rate on the sheet surface, on the other hand; the Lewis number and Brownian motion parameter cause a substantial increase in the Sherwood number (mass transfer rate).
- The Forchheimer parameter tends to escalate the $\chi'(0)$ on the surface of sheet.

References:

[1] Choi, S. U. S. "Enhancing thermal conductivity of fluids with nanoparticles developments and application of non-Newtonian flows", *ASME J. Heat Transfer*, **66,** pp. 99-105 (1997).

[2] Forchheimer, P., *Wasserbewegungduchbodenzeitschriftver ding*, **45**, pp. 1782-1788(1901).

[3] Muskat, M. "The flow of homogenous fluids through porous media", *MI: Edwards*, (1995).

[4] Seddeek, M. A. "Influence of viscous dissipation and thermophoresis on Darcy- Forchheimer mixed convection fluid in a saturated porous media", *J. Colloid. Interface Sci.*, **293**, pp. 137-142 (2006).

[5] Sajid, T., Sagheer, M., Hussain, S., et al. "Darcy-Forchheimer flow of Maxwell nanofluid with nonlinear thermal radiation and activation energy", *AIP Adv.*, **8**, https://doi.org/10.1063/1.5019218 (2018).

[6] Sheikholeslami, M. and Ebrahimpour, Z. "Nanofluid performance in a solar LFR system involving turbulator applying numerical simulation", *Adv. Powder Technol.*, **33**(8), https://doi.org/10.1016/j.apt.2022.103669 (2022).

[7] Sheikholeslami, M." Analyzing melting process of paraffin through the heat storage with honeycomb configuration utilizing nanoparticles", *J. Energy Storage*, **52**, https://doi.org/10.1016/j.est.2022.104954 (2022).

[8] Sheikholeslami, M."Numerical investigation of solar system equipped with innovative turbulator and hybrid nanofluid", *Sol. Energy Mater. Sol. Cells*, **243**, https://doi.org/10.1016/j.solmat.2022.111786 (2022).

[9] Saif, R. S., Hayat, T., Ellahi, R., et al. "Darcy-Forchheimer flow of nanofluid due to a curved stretching surface, International Journal of Numerical Methods", **29,** pp. 2-20 (2019).

[10] Nasir, S., Shah, Z., Islam, S., et al. "Darcy-Forchheimer nanofluid thin film flow of SWCNTs and heat transfer analysis over an unsteady stretching sheet", *AIP Adv.*, **9**, https://doi.org/10.1063/1.5083972 (2019).

[11] Khan, A., Shah, Z., Islam, S., et al. "Darcy-Forchheimer flow of MHD CNTs nanofluid radiative thermal behavior and convective non-uniform heat source/sink in the rotating frame with microstructure and inertial characteristics", *AIP Adv.*, **8**, https://doi.org/10.1063/1.5066223 (2018).

[12] Ganesh, N. V., Hakeem, A. K. A. and Ganga, B."Darcy-Forchheimer flow of hydromagnetic nanofluid over a stretching/shrinking sheet in a thermally stratified porous

medium with second order slip, viscous and Ohmic dissipation effects", *Ain Shams Eng. J.,* **9**, pp. 939-951 (2018).

[13] Hayat, T., Haider, F., Muhammad, T., et al. "Numerical study for Darcy-Forchheimer flow of nanofluid due to an exponentially stretching curved surface", *Results Phys.,* **8**, pp. 764-771 (2018).

[14] Sadiq, M. A. and Hayat, T."Darcy-Forchheimer flow of magneto Maxwell liquid bounded by convectively heated sheet", *Results Phys.,* **6**, pp. 884-890 (2016).

[15] Muhammad, T., Alsaedi, A., Shehzad, S. A., et al. "A revised model for Darcy-Forchheimer flow of Maxwell nanofluid subject to convective boundary condition", *Chinese J. Phys.,* **55**, pp. 963-976 (2017).

[16] Hayat, T., Aziz, A., Muhammad, T., et al. "Darcy-Forchheimer three-dimensional flow of nanofluid over a convectively nonlinear stretching surface", *Commun. Theor. Phys.,* **68,** https://doi.org/10.1088/0253-6102/68/3/387 (2017).

[17] Zakaullah, M., Capinnao S. S. and Baleanu, D. "A numerical simulation for Darcy-Forchheimer flow of nanofluid by a rotating disk with partial slip effects", *Front. Phys.,* **7**, https://doi.org/10.3389/fphy.2019.00219 (2020).

[18] Turk, O. and Sezin, M. T. "FEM solution to natural convection flow of a micropolar nanofluid in the presence of a magnetic field", *Meccanica*, **52**, pp. 889-901 (2017).

[19] Shafiq, A., Rasool, G. and Khalique, C. M. "Significance of thermal slip and convective boundary conditions in three dimensional rotating Darcy-Forchheimer nanofluid flow", *Symmetry*, **12,** http://dx.doi.org/10.3390/sym12050741 (2020).

[20] Saif, R. S., Hayat, T., Ellahi, R., et al. "Darcy-Forchheimer flow of nanofluid due to a curved stretching surface", *Int. J. Numer. Methods Heat Fluid Flow,* **29**, pp. 2-20 (2019).

[21] Nasir, S., Shah, Z., Islam, S., et al. "Darcy-Forchheimer nanofluid thin film flow of SWCNTs and heat transfer analysis over an unsteady stretching sheet", *AIP Adv.,* **9**, https://doi.org/10.1063/1.5083972 (2019).

[22] Rasool, G., Zhang, T., Chamka, A. J., et al. "Entropy generation and consequences of binary chemical reaction on MHD Darcy-Forchheimer Williamson nanofluid flow over nonlinearly stretching surface", *Entropy*, **22**, https://doi.org/10.3390/e22010018 (2020).

[23] Shahid, A., Zhou, Z., Hassan, M. et al. "Computational study of magnetized blood flow in the presence of gyrotactic microorganisms propelled through a permeable capillary in a stretching motion", *Int. J. Multiscale Comput. Eng.*, **16**, pp. 409-426 (2018).

[24] Waqas, H., Khan, S.U., Imran, M., et al. "Thermally developed Falkner-Skan bioconvection flow of a magnetized nanofluid in the presence of a motile gyrotactic microorganism: Buongiorno's nanofluid model", *Phys. Scr.*, **94**, https://doi.org/10.1088/1402-4896/ab2ddc (2019).

[25] Sohail, M. and Naz, R. "On the onset of entropy generation for a nanofluid with thermal radiation and gyrotactic microorganisms through three-dimensional flows", *Phys. Scr.*, **95**, https://doi.org/10.1088/1402-4896/ab3c3f (2020).

[26] Sheikholeslami, M. and Ebrahimpour, Z. "Thermal improvement of linear Fresnel solar system utilizing Al_2O_3-water nanofluid and multi-way twisted tape", *Int. J. Therm. Sci.*, **176**, https://doi.org/10.1016/j.ijthermalsci.2022.107505 (2022).

[27] Sheikholeslami, M., Said, Z. and Jafaryar, M. "Hydrothermal analysis for a parabolic solar unit with wavy absorber pipe and nanofluid", *Renew. Energy*, **188**, pp. 922-932 (2022).

[28] Sheikholeslami, M., Jafaryar, M., Gerdroodbary, M. B., et al. "Influence of novel turbulator on efficiency of solar collector system", *Environ. Technol. Innov.*, **26**, https://doi.org/10.1016/j.eti.2022.102383 (2022).

[29] Sheikholeslami, M. and Farshad, S. A., et al. "Nanoparticles transportation with turbulent regime through a solar collector with helical tapes", *Adv. Powder Technol.*, **33**(3), https://doi.org/10.1016/j.apt.2022.103510 (2022).

[30] Ahmad, S., Younis, J., Ali, K., et al. "Impact of swimming gyrotactic microorganisms and viscous dissipation on nanoparticles flow through a permeable medium- a numerical assessment", J. Nanomater., **2022**, https://doi.org/10.1155/2022/4888128 (2022).

[31] Ahmad, S., Akhter, S., Shahid, M. I., et al. "Novel thermal aspects of hybrid nanofluid flow comprising of manganese zinc ferrite $MnZnFe_2O_4$, nickel zinc ferrite $NiZnFe_2O_4$ and motile microorganisms, *Ain Shams Eng. J.*, **13**(5): https://doi.org/10.1016/j.asej.2021.101668 (2022).

[32] Akhter, S., Ahmad, S. and Ashraf, M. "Cumulative impact of viscous dissipation and heat generation on MHD Darcy-Forchheimer flow between two stretchable disks: Quasi linearization technique", *J. Sci. Arts*, **22**(1), pp. 219-232, (2022).

[33] Shahid, M. I., Ahmad, S. and Ashraf, M. “Simulation analysis of mass and heat transfer attributes in nanoparticles flow subject to Darcy-Forchheimer medium”, *Sci. Iran.*, DOI: 10.24200/SCI.2022.58552.5786 (2022).

[34] Ahmad, S., Ali, K., Haider, T., et al. “Thermal characteristics of kerosene oil-based hybrid nanofluids (Ag-$MnZnFe_2O_4$): A comprehensive study”, *Front. Energy Res.*, DOI:10.3389/fenrg.2022.978819 (2022).

[35] Ali, K., Ahmad, S., Baluch, O., et al. “Numerical study of magnetic field interaction with fully developed flow in a vertical duct”, *Alex. Eng. J.*, **61**(12), pp. 11351–11363 (2022).

[36] Rasool, G., Shafiq, A., Khalique, C.M., et al. “MHD Darcy-Forchheimer nanofluid flow over a nonlinear stretching sheet”, *Phys. Scr.*, **94**(10), https://doi.org/10.1088/1402-4896/ab18c8 (2014).

List of Figures Captions:

Fig. 1: The geometry of the flow problem

Fig. 2: Velocity distribution for different values of Me by setting $\lambda = 0.2, Fr = 0.2, \Pr = 1.2, Nb = 0.1, Nt = 0.2, m = 1.3, Ec = 0.1, \sigma_{Ec} = 0.2, Le = 2, Pe = 0.1 \,\&\, Sc = 2.2.$

Fig. 3: Microorganism’s density distribution for different values of Me by setting $\lambda = 0.2, Fr = 0.2, \Pr = 1.2, Nb = 0.1, Nt = 0.2, m = 1.3, Ec = 0.1, \sigma_{Ec} = 0.2, Le = 2, Pe = 0.1 \,\&\, Sc = 2.2.$

Fig. 4: Microorganism’s concentration for different values of Me by setting $\lambda = 0.2, Fr = 0.2, \Pr = 1.2, Nb = 0.1, Nt = 0.2, m = 1.3, Ec = 0.1, \sigma_{Ec} = 0.2, Le = 2, Pe = 0.1 \,\&\, Sc = 2.2.$

Fig. 5: Temperature distribution for different values of Me by setting $\lambda = 0.2, Fr = 0.2, \Pr = 1.2, Nb = 0.1, Nt = 0.2, m = 1.3, Ec = 0.1, \sigma_{Ec} = 0.2, Le = 2, Pe = 0.1 \,\&\, Sc = 2.2.$

Fig. 6: Velocity distribution for various values of λ by setting $Me = 0.3, Fr = 0.2, \Pr = 2.2, Nb = 0.1, Nt = 0.2, m = 1.3, Ec = 0.1, \sigma_{Ec} = 0.2, Le = 1.9, Pe = 0.1 \,\&\, Sc = 2.$

Fig. 7: Microorganisms’ density distribution for various values of λ by setting $Me = 0.3, Fr = 0.2, \Pr = 2.2, Nb = 0.1, Nt = 0.2, m = 1.3, Ec = 0.1, \sigma_{Ec} = 0.2, Le = 1.9, Pe = 0.1 \,\&\, Sc = 2.$

Fig. 8: Temperature distribution for various values of λ by setting $Me = 0.3, Fr = 0.2, \Pr = 2.2, Nb = 0.1, Nt = 0.2, m = 1.3, Ec = 0.1, \sigma_{Ec} = 0.2, Le = 1.9, Pe = 0.1 \,\&\, Sc = 2.$

Fig. 9: Microorganism’s concentration for various values of λ by setting $Me = 0.3, Fr = 0.2, \Pr = 2.2, Nb = 0.1, Nt = 0.2, m = 1.3, Ec = 0.1, \sigma_{Ec} = 0.2, Le = 1.9, Pe = 0.1 \,\&\, Sc = 2.$

Fig. 10: Velocity distribution for various values of Fr by setting $Me = 0.3, \lambda = 0.2, \Pr = 1.2, Nb = 0.1, Nt = 0.2, m = 1.3, Ec = 0.1, \sigma_{Ec} = 0.2, Le = 2, Pe = 0.1 \,\&\, Sc = 2.2.$

Fig. 11: Microorganism’s density distribution for various values of Fr by setting

$Me = 0.3, \lambda = 0.2, \Pr = 1.2, Nb = 0.1, Nt = 0.2, m = 1.3, Ec = 0.1, \sigma_{Ec} = 0.2, Le = 2, Pe = 0.1 \& Sc = 2.2.$

Fig. 12: Temperature distribution for various values of Fr by setting $Me = 0.3, \lambda = 0.2, \Pr = 1.2, Nb = 0.1, Nt = 0.2, m = 1.3, Ec = 0.1, \sigma_{Ec} = 0.2, Le = 2, Pe = 0.1 \& Sc = 2.2.$

Fig. 13: Microorganism's concentration for various values of Fr by setting $Me = 0.3, \lambda = 0.2, \Pr = 1.2, Nb = 0.1, Nt = 0.2, m = 1.3, Ec = 0.1, \sigma_{Ec} = 0.2, Le = 2, Pe = 0.1 \& Sc = 2.2.$

List of Tables Captions:

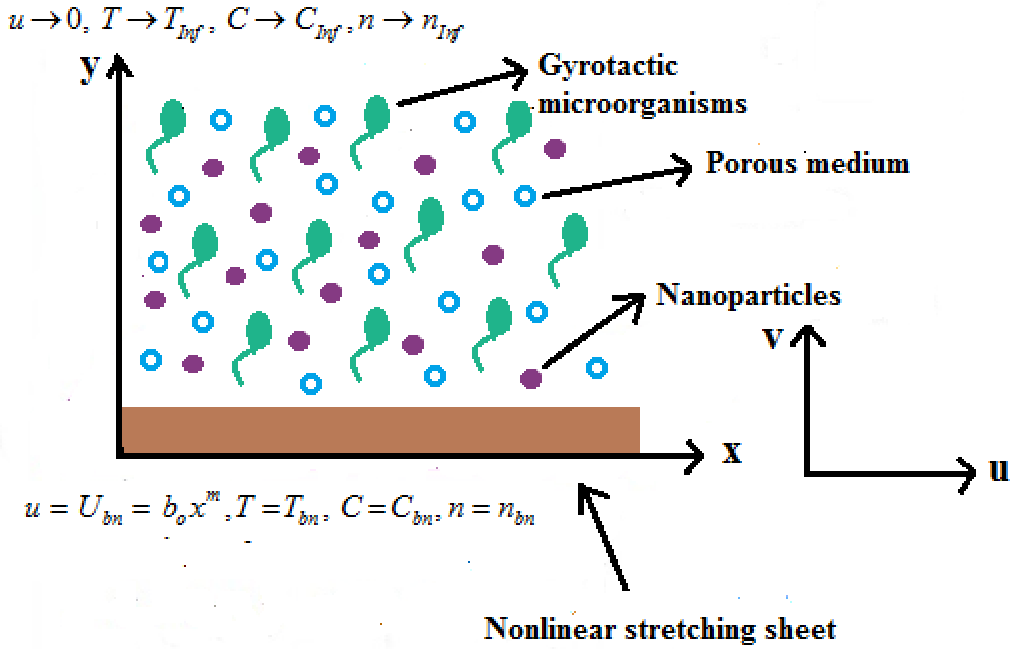

Fig. 1: The geometry of the flow problem

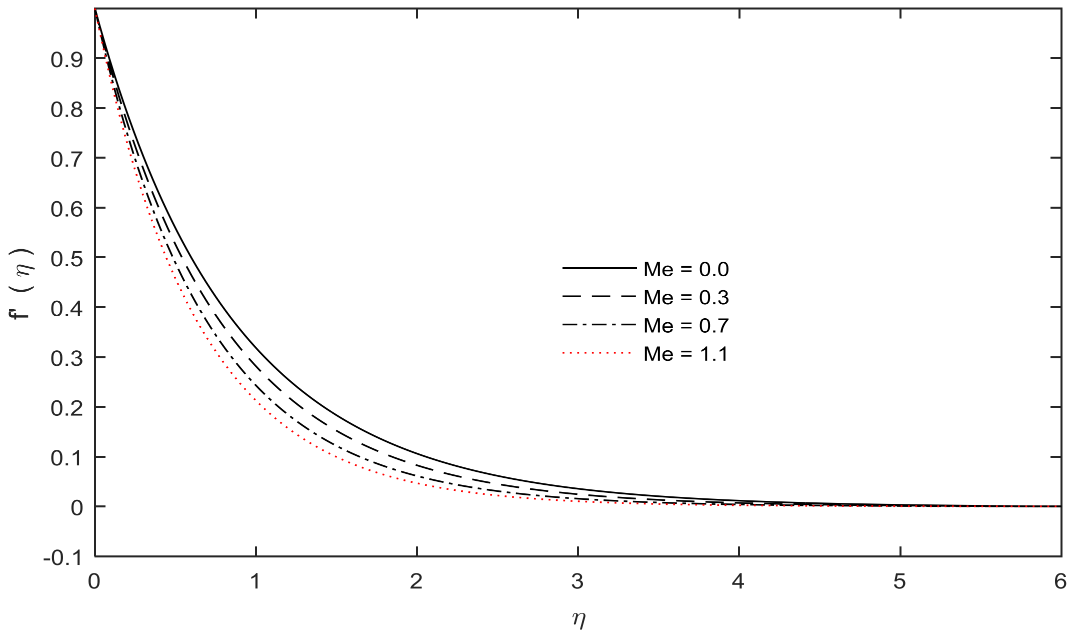

Fig. 2: Velocity distribution for different values of *Me* by setting $\lambda = 0.2, Fr = 0.2, \Pr = 1.2, Nb = 0.1, Nt = 0.2, m = 1.3, Ec = 0.1, \sigma_{Ec} = 0.2, Le = 2, Pe = 0.1 \,\&\, Sc = 2.2.$

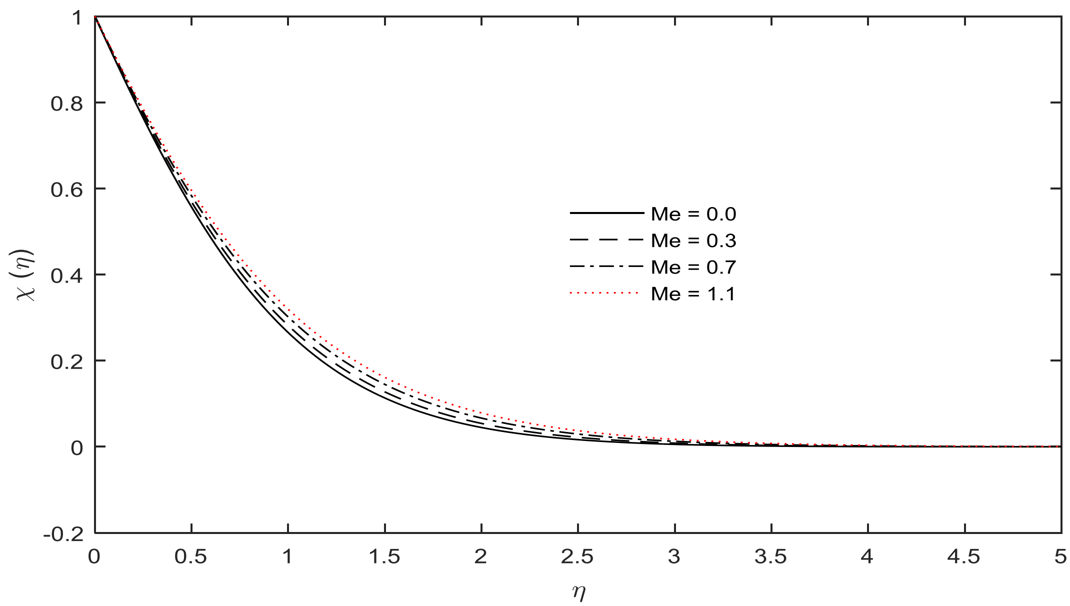

Fig. 3: Microorganism's density distribution for different values of *Me* by setting $\lambda = 0.2, Fr = 0.2, \Pr = 1.2, Nb = 0.1, Nt = 0.2, m = 1.3, Ec = 0.1, \sigma_{Ec} = 0.2, Le = 2, Pe = 0.1 \,\&\, Sc = 2.2.$

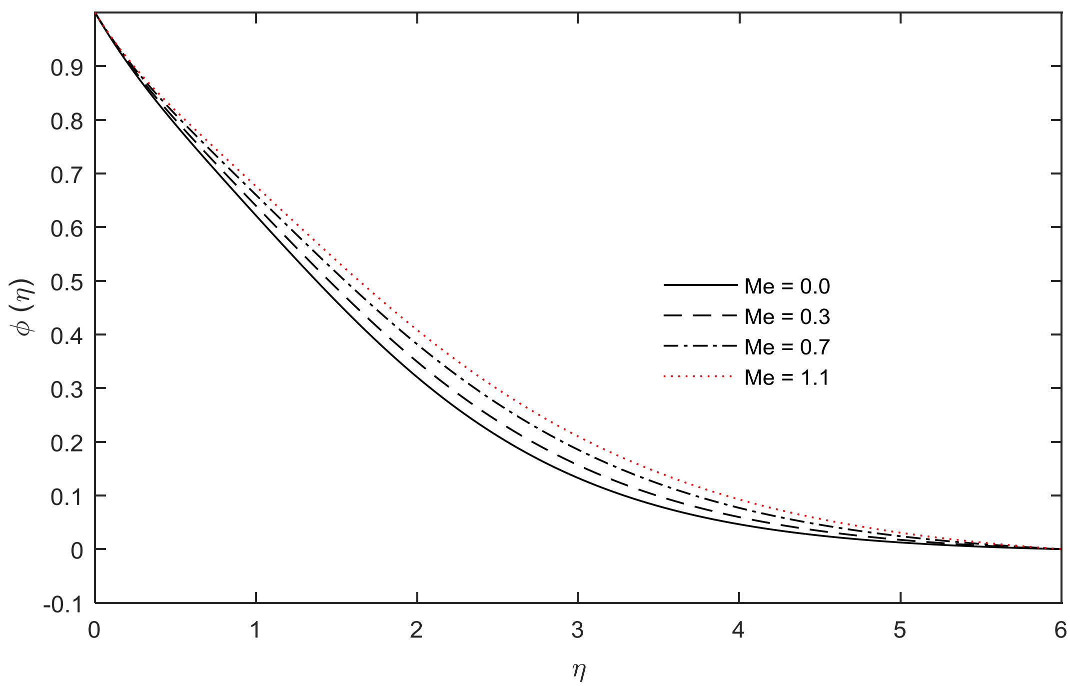

Fig. 4: Microorganism's concentration for different values of *Me* by setting $\lambda = 0.2, Fr = 0.2, \Pr = 1.2, Nb = 0.1, Nt = 0.2, m = 1.3, Ec = 0.1, \sigma_{Ec} = 0.2, Le = 2, Pe = 0.1 \;\&\; Sc = 2.2.$

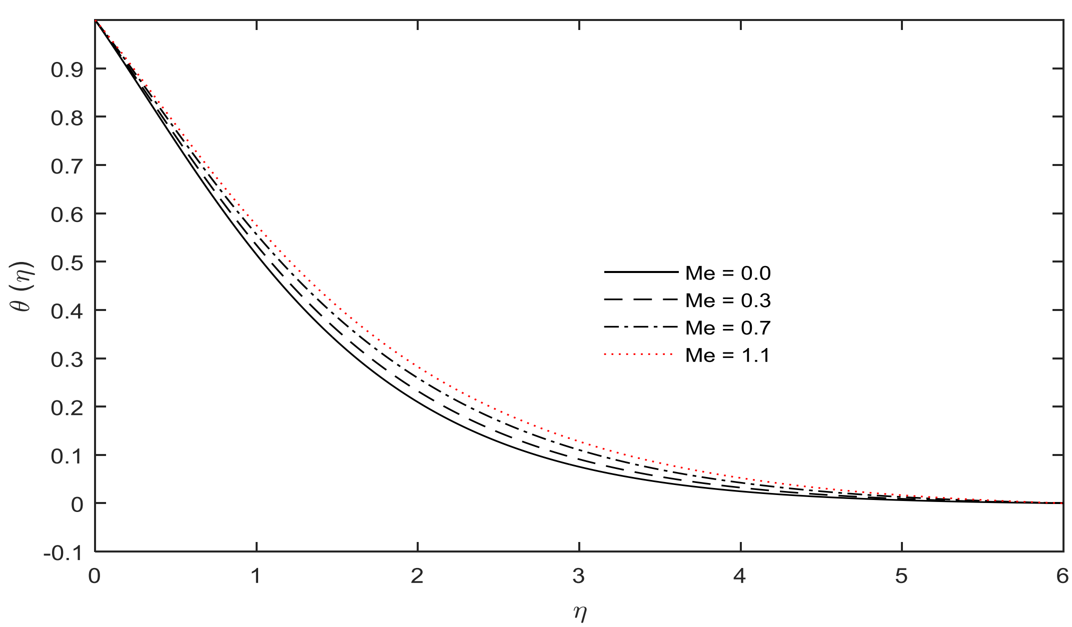

Fig. 5: Temperature distribution for different values of *Me* by setting $\lambda = 0.2, Fr = 0.2, \Pr = 1.2, Nb = 0.1, Nt = 0.2, m = 1.3, Ec = 0.1, \sigma_{Ec} = 0.2, Le = 2, Pe = 0.1 \;\&\; Sc = 2.2.$

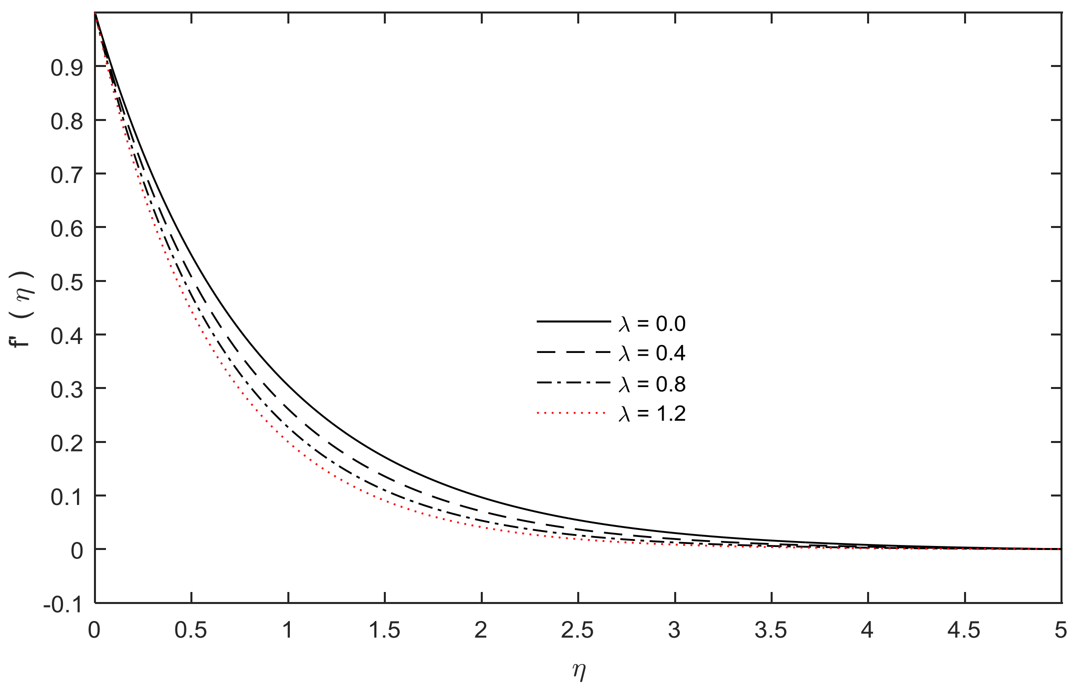

Fig. 6: Velocity distribution for various values of λ by setting $Me = 0.3, Fr = 0.2, \Pr = 2.2, Nb = 0.1, Nt = 0.2, m = 1.3, Ec = 0.1, \sigma_{Ec} = 0.2, Le = 1.9, Pe = 0.1 \& Sc = 2.$

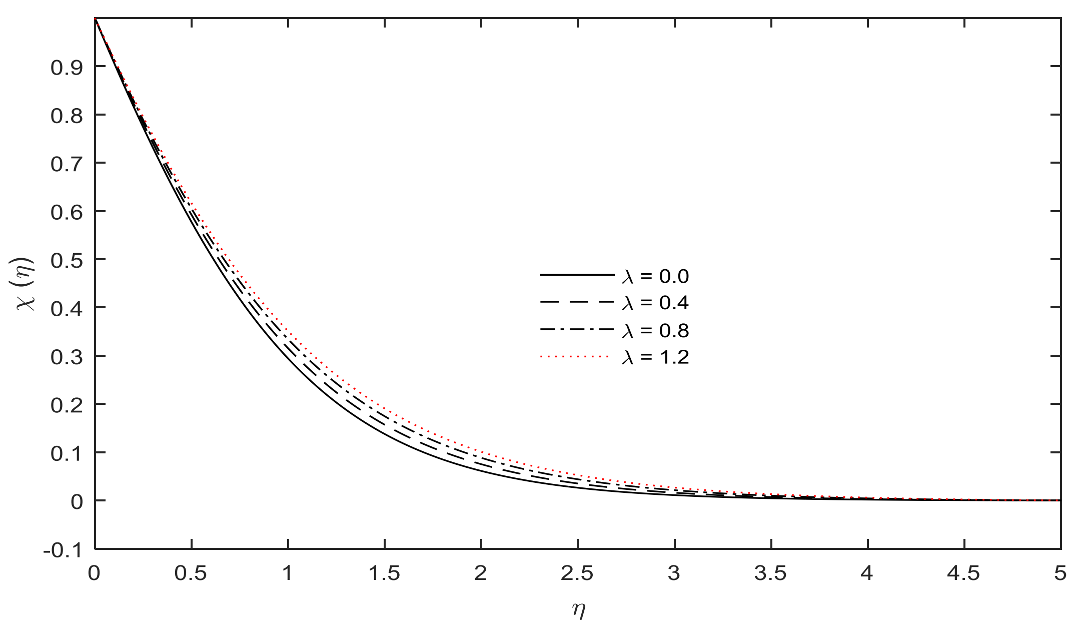

Fig. 7: Microorganisms' density distribution for various values of λ by setting $Me = 0.3, Fr = 0.2, \Pr = 2.2, Nb = 0.1, Nt = 0.2, m = 1.3, Ec = 0.1, \sigma_{Ec} = 0.2, Le = 1.9, Pe = 0.1 \& Sc = 2.$

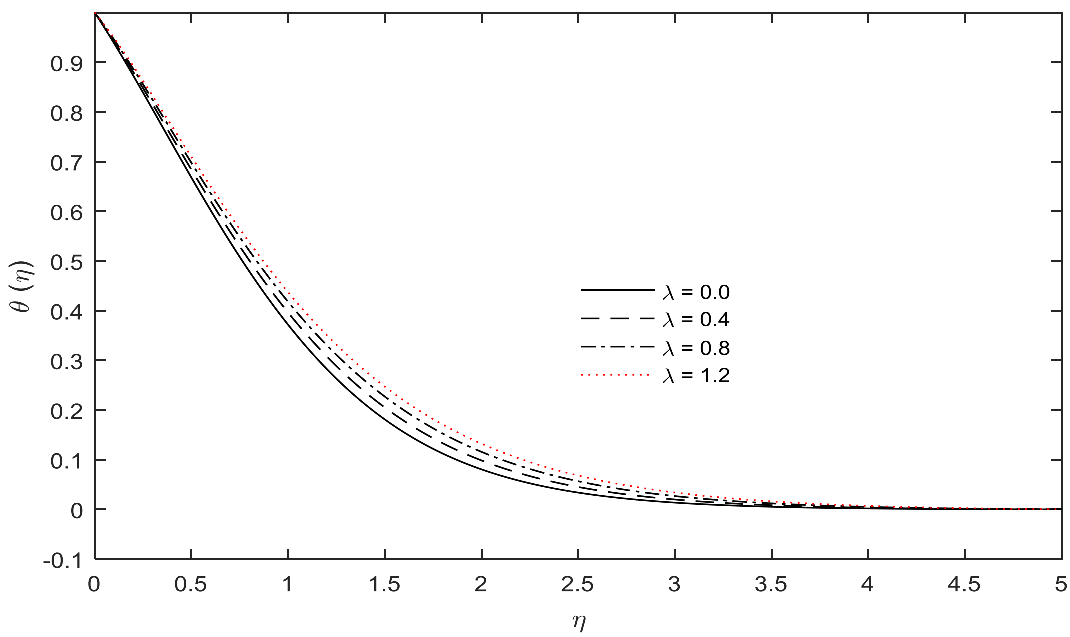

Fig. 8: Temperature distribution for various values of λ by setting $Me=0.3, Fr=0.2, \Pr=2.2, Nb=0.1, Nt=0.2, m=1.3, Ec=0.1, \sigma_{Ec}=0.2, Le=1.9, Pe=0.1 \,\&\, Sc=2.$

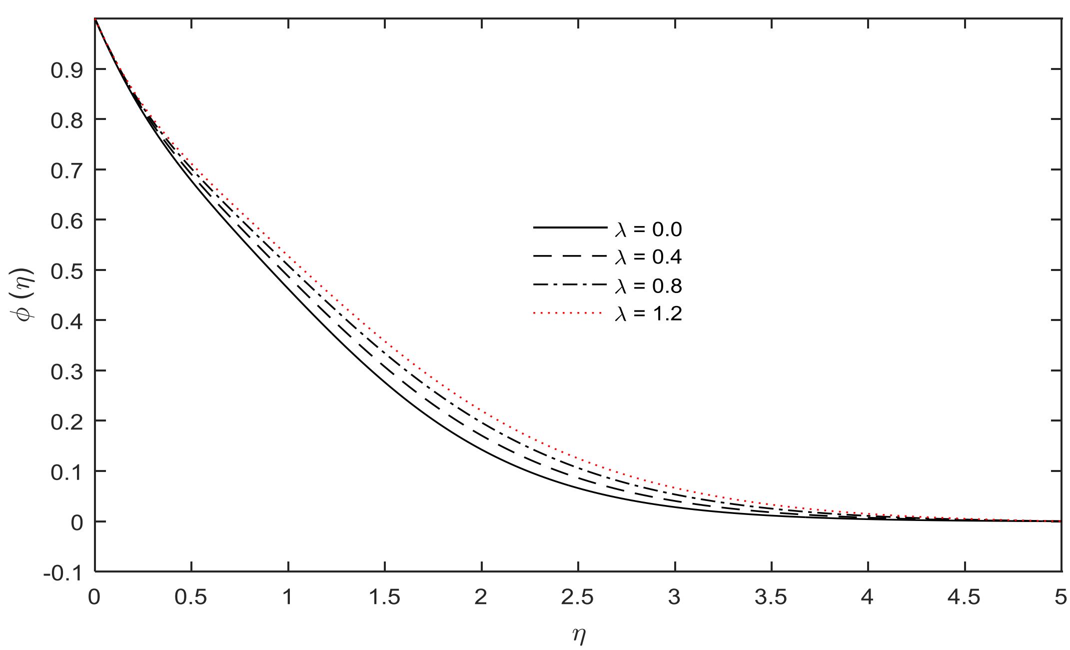

Fig. 9: Microorganism's concentration for various values of λ by setting $Me=0.3, Fr=0.2, \Pr=2.2, Nb=0.1, Nt=0.2, m=1.3, Ec=0.1, \sigma_{Ec}=0.2, Le=1.9, Pe=0.1 \,\&\, Sc=2.$

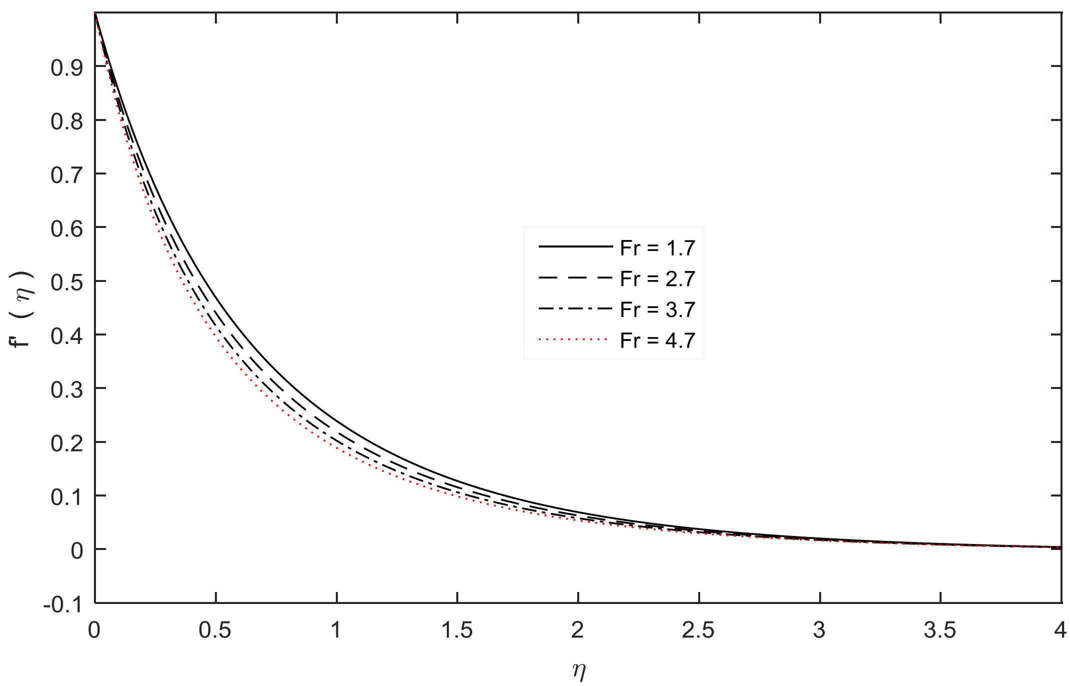

Fig. 10: Velocity distribution for various values of *Fr* by setting $Me = 0.3, \lambda = 0.2, \Pr = 1.2, Nb = 0.1, Nt = 0.2, m = 1.3, Ec = 0.1, \sigma_{Ec} = 0.2, Le = 2, Pe = 0.1 \& Sc = 2.2.$

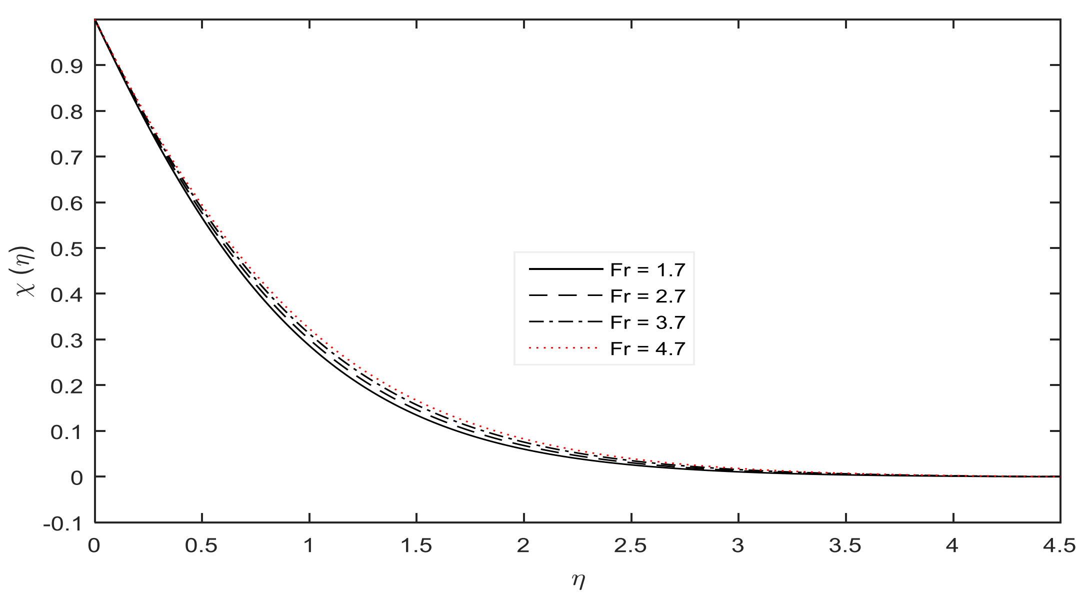

Fig. 11: Microorganism's density distribution for various values of *Fr* by setting $Me = 0.3, \lambda = 0.2, \Pr = 1.2, Nb = 0.1, Nt = 0.2, m = 1.3, Ec = 0.1, \sigma_{Ec} = 0.2, Le = 2, Pe = 0.1 \& Sc = 2.2.$

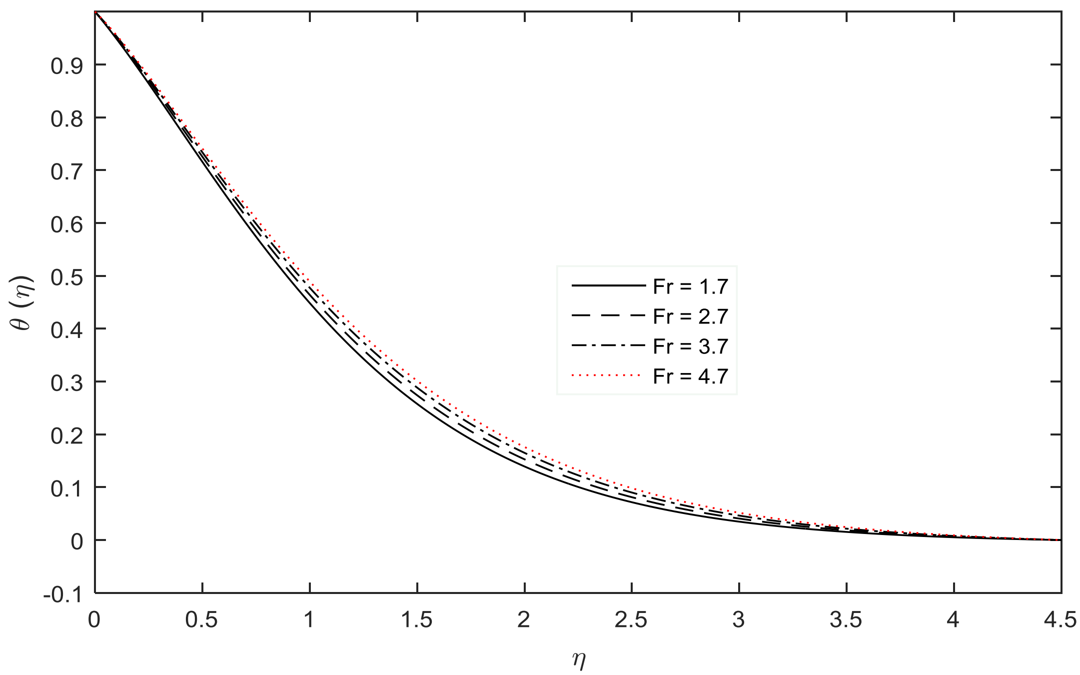

Fig. 12: Temperature distribution for various values of Fr by setting $Me = 0.3, \lambda = 0.2, \Pr = 1.2, Nb = 0.1, Nt = 0.2, m = 1.3, Ec = 0.1, \sigma_{Ec} = 0.2, Le = 2, Pe = 0.1 \& Sc = 2.2.$

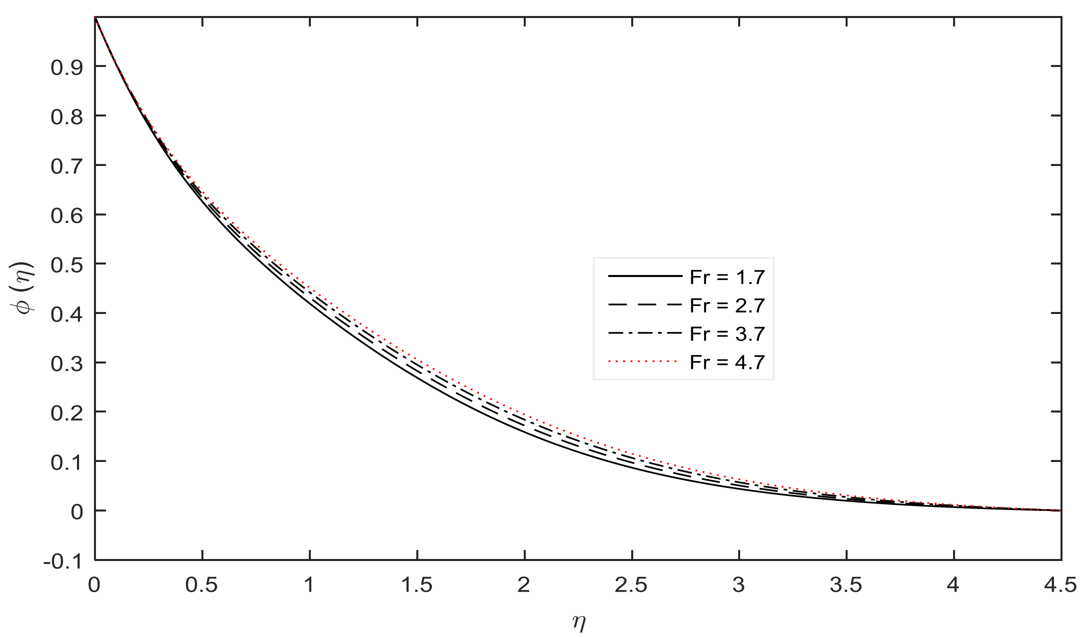

Fig. 13: Microorganism's concentration for various values of Fr by setting $Me = 0.3, \lambda = 0.2, \Pr = 1.2, Nb = 0.1, Nt = 0.2, m = 1.3, Ec = 0.1, \sigma_{Ec} = 0.2, Le = 2, Pe = 0.1 \& Sc = 2.2.$

Table 1. Comparison with Rasool et al. [36] by setting $Ec = 0, \sigma_{Ec} = 0, Pe = 0 \& Sc = 0.$

Fr	$-\mathrm{Re}_x^{-1/2} Nu_x$		$-\mathrm{Re}_x^{-1/2} Sh_x$	
	Present	Rasool et al. [36]	Present	Rasool et al. [36]
0.0	0.5133	0.5115	0.4088	0.4085
0.6	0.4936	0.4953	0.3767	0.3925
1.2	0.4853	0.4814	0.3728	0.3789

Table 2. Variation in $f''(0)$, for diverse values of λ, Fr and Me.

λ	Me	Fr	$f''(0)$
0.0	0.2	0.9	-1.423938
0.3			-1.53581
0.5			-1.606089
0.2	0.0	0.9	-1.423938
	0.2		-1.499455
	0.4		-1.571352
0.2	0.2	0.0	-1.267705
		0.3	-1.349067
		0.6	-1.426118

Table 3. Variation in $-\theta'(0)$, against various values of Nt, Nb, λ, Fr, Ec and Me.

Nt	Nb	λ	Fr	Ec	Me	$-\theta'(0)$
0.1	0.2	0.2	0.9	0.1	0.2	0.445417
0.2						0.415899
0.4						0.385252
0.1	0.1	0.2	0.9	0.1	0.2	0.467118
	0.2					0.432433
	0.4					0.391482
0.1	0.2	0.0	0.9	0.1	0.2	0.456385
		0.3				0.426793
		0.5				0.414351
0.1	0.2	0.2	0.0	0.1	0.2	0.466133
			0.3			0.446389
			0.6			0.437961
0.1	0.2	0.2	0.9	0.0	0.2	0.499539
				0.1		0.431806
				0.2		0.376081
0.1	0.2	0.2	0.9	0.1	0.0	0.456385
					0.2	0.432169
					0.4	0.419783

Table 4. Variation in $-\phi'(0)$, for diverse values of Me, λ, Nb, Nt, Le and Fr.

Me	λ	Le	Nb	Nt	Fr	$-\phi'(0)$
0.0	0.2	0.8	0.2	0.1	0.9	0.430925
0.2						0.401441
0.4						0.397490
0.2	0.0	0.8	0.2	0.1	0.9	0.430925
	0.3					0.400779
	0.5					0.396747
0.2	0.2	0.3	0.2	0.1	0.9	0.307160
		0.5				0.311506
		0.7				0.363977
0.2	0.2	0.8	0.1	0.1	0.9	0.328577
			0.2			0.392125
			0.4			0.447677
0.1	0.2	0.8	0.2	0.1	0.9	0.429622
				0.2		0.335406
				0.4		0.237252
0.2	0.2	0.8	0.7	0.1	0.0	0.431477
					0.3	0.402987
					0.6	0.399828

Table 5. Variation in $-\chi'(0)$, for diverse values of Me, λ, Pe, Sc and Fr.

Me	λ	Pe	Sc	Fr	$-\chi'(0)$
0.0	0.2	0.2	0.3	0.9	0.455078
0.2					0.416871
0.4					0.410072
0.2	0.0	0.2	0.3	0.9	0.455078
	0.3				0.415472
	0.5				0.408550
0.2	0.2	0.1	0.3	0.9	0.422488
		0.3			0.442529
		0.5			0.498732
0.2	0.2	0.2	0.1	0.9	0.398371
			0.3		0.411313
			0.5		0.470771
0.2	0.2	0.2	0.3	0.0	0.457298
				0.3	0.420555
				0.6	0.415024

Biographies

Maria Batool

Maria Batool is PhD Scholar under the supervision of Professor Dr. Muhammad Ashraf and Dr. Kashif Ali at the Centre for Advanced Studies in Pure and Applied Mathematics, Bahauddin Zakariya University, Multan, Pakistan.

Shaheen Akhter

Shaheen Akhter recently completed her PhD in mathematics under the supervision of Professor Dr. Muhammad Ashraf in the Centre for Advanced Studies in Pure and Applied Mathematics, Bahauddin Zakariya University, Multan, Pakistan. She is Lecturer at COMSATS University Islamabad, (Sahiwal Campus), Pakistan.

Sohail Ahmad

Sohail Ahmad has recently completed his PhD in Applied Mathematics from Centre for Advanced Studies in Pure and Applied Mathematics, Bahauddin Zakariya University, Multan 60800, Pakistan. He is working as visiting faculty member at the Department of Mathematics, Muhammad Nawaz Sharif University of Engineering and Technology, Multan, Pakistan. His doctoral research investigates the heat and mass transfer, computational fluid dynamics, thermal analysis, advances in nanofluids, numerical study of flows through porous media and magnetohydrodynamics. He takes a multidisciplinary approach that encompasses the fields of Applied Mathematics, Bio-mechanics, Fluid Mechanics, Mathematical physics and Mechanics. He is potential reviewer of several international journals. Recently, he authored more than twenty publications.

Kashif Ali

Kashif Ali received the PhD Degree from Bahauddin Zakariya University, Multan 60800, Pakistan. He is working as an Assistant Professor in the department of mathematics, Muhammad Nawaz Sharif University of engineering and Technology, Multan, Pakistan. He has numerous publications (more than 50) on his account in conferences and impact factor international journals. He is actively involved in Numerical Simulation of the fluid flow problems. Recently, He developed various numerical methods such as Successive over Relaxation Method, Finite Element Method, Quasi-linearization Method and successive under Relaxation method in his publications. His research interests include Multiphase Fluid-Particle Dynamics, Energy Systems Modeling, Nanofluids Flow Modeling.

Muhammad Ashraf

Muhammad Ashraf is working as a Professor at the Centre for Advanced Studies in Pure and Applied Mathematics, Bahauddin Zakariya University, Multan, Pakistan. He has numerous publications (more than 70) on his account in impact factor international journals. He is actively involved in Numerical Simulation of the fluid flow problems. He has supervised and co-supervised many students of M. Phil and PhD. His research interests include Fluid-Particle Dynamics, Nanofluids Flow Modeling, Transport in Porous Media, Heat and Mass Transfer, Magnetohydrodynamics, Numerical Analysis, Fluid-Particle Separation, Heat and Fluids, Computational Fluid Dynamics, Modeling of fluid flow problems, Nonlinear Science, Nanofluid, Ferrohydrodynamic, Electrohydrodynamic and Numerical Simulation of Mathematical Models.